SASEC
1st Southern African Solar Energy Conference
21-23 May 2012

ROCK BED STORAGE BASED SIMULATION OF A 5MWe COMBINED CYCLE SOLAR POWER PLANT

Lukas Heller[1] and Paul Gauché[2]

[1] Diplomate, TU Dresden, Germany / Research Affiliate, Solar Thermal Energy Research Group, Stellenbosch University, E-mail: Lukas_Heller@gmx.de

[2] MEng (Mech) Sr. Researcher and Coordinator of the Solar Thermal Energy Research Group, Stellenbosch University, Private Bag X1, Matieland, 7602, South Africa, Phone: +27 21 808 4242, E-mail: paulgauche@sun.ac.za

Abstract

A rock bed thermal energy storage system potentially offers a cheaper and simpler way of achieving dispatchability in a central receiver CSP plant. In order to efficiently match heliostat field size, storage dimensions, back-up fuel consumption and turbine sizes for non-stop power generation and economic feasibility, a simulation model of the whole power plant has to be created. This paper focuses on the storage as the center of in- and outgoing heat fluxes. The derived storage model has one spatial dimension which is justified by the high tube-to-particle diameter ratio. A validation of the correlations shows reasonably accurate results. These will have to be confirmed once simulations for the whole plant are run.

Keywords: CSP; Thermal Energy Storage; Packed Bed; Rock Bed; Simulation

Nomenclature

$c_{(p)}$	specific heat capacity (at constant pressure) [J/(kg K)]	Δp	pressure drop [N/m^2]
D	diameter of storage tank [m]	Δx	vertical length of one layer [m]
d_p	equivalent particle diameter [m]	ε	bed void fraction [-]
G	mass flux [kg/(m^2 s)]	λ	thermal conductivity [W/(m K)]
$Hg = \rho_f \frac{\Delta p_i}{\Delta x} \frac{{d_p}^3}{{\mu_f}^2}$	Hagen number [-]	μ	dynamic viscosity [kg/(s m)]
L	vertical length of tank [m]	ρ	density [kg/m^3]
m	mass [kg]	τ	time [s]
$\dot{m}$	mass flow [kg/s]	$\tau_{NTU,i,j} = \frac{m_s c_s}{\dot{m}_f c_{p,f}}$	time constant of bed [s]
$N=D/d_p$	tube-to-particle diameter ratio [-]	ψ	sphericity of particles [-]
$NTU(^*)$	(apparent) Number of Transfer Units [-]	Subscripts	
Pr	Prandtl number [-]	e	electric
$\dot{Q}_{loss}$	heat flux of losses [W]	eff	effective
$Re_p=G\,d_p/\mu_f$	particle Reynolds number [-]	f	fluid
$T\,/\,t$	temperature [K] / [°C]	i	vertical step i
α	heat transfer coefficient [W/(m^2 K)]	j	time step j
α_v	volumetric heat transfer coefficient [W/(m^3 K)]	s	solid

1. Introduction

The necessity to shift from conventional power generation - mostly from fossil fuels - towards the use of renewable energy sources is widely acknowledged. Some of the reasons for this are the climate change, irreparable damages to the environment and the scarcity of fossil and nuclear fuels. The latter possibly leading to collapsing economies and political as well as social conflicts.

Of all the renewable energies, solar is by far the most abundant and South Africa is one of the prime locations world-wide. Concentrating Solar Power (CSP) offers the unique possibility of easy energy storage solutions due to the conversion of solar into thermal energy.

A central receiver CSP plant promises the highest efficiencies of all solar technologies due to the elevated temperatures. For fully using this concept, the combined cycle, as known from natural gas fired plants, has the best potential. Figure 1 shows the Stellenbosch University Solar Power Thermodynamic (SUNSPOT) cycle. It features a central air receiver with an additional combustion chamber that power the gas turbine. The hot exhaust gas supplies the steam cycle's boiler and/or charges the thermal energy storage (TES). In discharging mode, a blower forces gas through the storage and boiler. The advantages of this layout are:

- High efficiency due to combined cycle
- Safe back-up solution by additional burner
- Dispatchability of power to evening peaks or night times by TES system
- No expensive heat transfer fluid (HTF) or storage medium needed
- Constant temperatures and ramp ups in the heat exchanger and steam turbine
- Possibility to run steam cycle at night with increased cooling efficiency

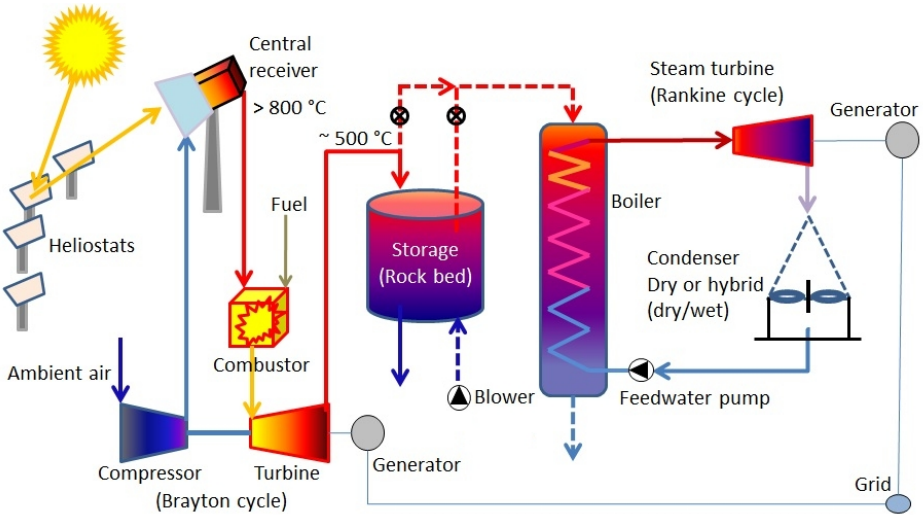

Figure 1: SUNSPOT cycle. Graphic by Kröger [1] with own changes

A packed bed of rocks has been chosen as the TES. Besides the very low estimated costs of a tank filled with abundant rocks as compared to any other storage material, the system also doesn't need any additional heat exchanger and is environmentally uncritical.

The goal of the described simulation is to find economically optimized configurations of heliostat field size, turbine sizes, fuel firing, storage dimensions and design.

2. Literature Review on Packed Beds

The heat transfer and fluid flow characteristics in packed beds have been subject to many studies over the last decades. The 'classical' analytical solution for heat transfer between a fluid and solids in a packed bed was developed by Schumann [2], his main assumptions being: (a) High thermal conductivity inside the solids, (b) little conductivity between solids in axial direction, (c) constant fluid properties, (d) no wall heat losses, (e) plug flow and (f) no temperature gradient in radial direction. One further simplification is neglecting the thermal capacitance of the fluid which leads to the Effectiveness-Number of Transfer Units (or E-NTU) method as introduced by Hughes [3]. It simplifies the differential equations of the Schumann model and includes a term for heat losses to the surroundings.

In order to describe heat transfer more realistically, later studies usually relaxed one or several of these assumptions. Assumption (a) leads to constant temperatures inside each solid element. This can be relaxed by using a corrected value for the NTU, taking into consideration the time until a surface temperature change reaches the center of a solid, as done by Sagara and Nakahara [4].

Obtaining the heat transfer coefficient between solid and fluid is the NTU method's major challenge and there are numerous empirical equations for it. Martin [5] proposed in his version of the Generalized Lévêque Equation (GLE) a dependency of the heat transfer on the pressure drop over the bed. Allen [6] verified this method with wind tunnel test for different rocks at low temperatures.

The pressure drop of a thermal storage not only determines the power required for charge and discharge. Heat transfer between fluid and solids as well as the axial and radial temperature distributions are also greatly influenced by it.

In real world packed beds, there will always be radial flows, perpendicular to the main flow direction. This combined with different flow speeds in the main flow direction creates temperature gradients in the radial dimension. The latter is caused by the uneven contribution of void fractions in the bed (so called wall effect), friction at the outside walls and uneven flow profiles at in- and outlet. The magnitude of flow uniformity is not being agreed on but most studies (e.g [7]) concluded that the smaller density of solids next to the wall leads to a much higher superficial fluid velocity there. Allen used wall linings to avoid high void fractions near the walls of the tanks.

Singh, Saini and Saini [8] stated that if small particles are used, the pressure drop has to be increased in order to achieve a uniform flow distribution. They tested particles of different shapes and developed a pressure drop correlation considering the 'sphericity' ψ of the particles. Zunft, Hahn, Kammel [9] did CFD simulations to optimize inlet and outlet designs for uniform flow profiles.

3. Charging/Discharging

All fluid properties (density, thermal conductivity, viscosity, heat capacity) are calculated for every time step by use of polynomial approximations because of the changing temperatures. They were found to differ at least 10 % in the temperature range of interest so that the additional computational time is justified.

The simulated storage system will have a cylindrical tank of considerable size ($D,L>5$ m) that is charged from the top and discharged from the bottom. 'Wall channeling' will be considered negligible because of the high tube-to-particle diameter ratio N, a flow distribution system at the inlets and possibly wall linings. Two articles [10] and [11] state that this is justified at N values bigger than 40 or 20, respectively. If, additionally to the assumption described above, high radial thermal conductivities as well as low heat losses through the walls because of insulation material are assumed, the use of a one-dimensional model is valid.

Equations (1) and (2) are derived from the E-NTU approach by Allen [6] when adding heat losses. The procedure is to calculate the temperature of the air entering the next section ($i+1$th) of the bed assuming an exponential temperature distribution inside each section. The next step is to find the solids' temperature at the

next *time*-step *j+1* by applying energy conservation formulas. The time constant τ_{NTU} has been substituted for simplification purposes.

$$T_{f,i+1} = T_{f,i} - \left(T_{f,i} - T_{s,i}\right)\overbrace{\left(1 - e^{-NTU_i\frac{\Delta x}{L}}\right)}^{\eta_i} - \frac{\dot{Q}_{loss,i}}{\dot{m}_f c_{p,f,i}} \tag{1}$$

$$T_{s,i,j+1} = \frac{T_{s,i,j}\left(1 - \frac{1}{2}\left[\frac{\Delta\tau\, L\, \eta_{i,j}}{\Delta x\, \tau_{NTU,i,j}}\right]\right) + T_{f,i,j}\left[\frac{\Delta\tau\, L\, \eta_{i,j}}{\Delta x\, \tau_{NTU,i,j}}\right]}{1 + \frac{1}{2}\left[\frac{\Delta\tau\, L\, \eta_{i,j}}{\Delta x\, \tau_{NTU,i,j}}\right]} \tag{2}$$

Instead of the classic NTU term, the corrected NTU* term by Sagara and Nakahara [4] is used. This accounts for temperature gradients inside large particles and is derived from Equation (3). The uncorrected term is calculated according to Hughes [3] in Equation (4).

$$NTU^* = NTU\frac{20}{3\frac{\alpha_v {d_p}^2}{4\lambda_s(1-\varepsilon)} + 20} \tag{3}$$

$$NTU = \alpha_v \frac{A_{cs}L}{\dot{m}_f\, c_{p,f}} \tag{4}$$

The volumetric heat transfer coefficient α_v can be derived from the heat transfer coefficient per surface area α and the specific surface area of the bed per unit volume A_v. Equation (5) is technically only valid for spheres and cubes but is sufficiently accurate for other shapes of rocks as well since the calculations are already based on an equivalent particle diameter d_p.

$$\alpha_v = \alpha\, A_v = \alpha\, \frac{6\,(1-\varepsilon)}{d_p} \tag{5}$$

Finally, finding the correct correlation for this heat transfer coefficient might be the biggest challenge in the process. Out of the many different approaches in the literature, the GLE from Martin [5] has been chosen because it has been compared favorably by Allen [6] to rocks with the properties looked for. The governing equations of the method are (6) and (7).

$$\alpha = 0.4038\frac{\lambda_f}{d_p}\left[2\, x_f\, Hg\, \frac{d_h}{L_f} Pr\right]^{1/3} \tag{6}$$

$$\frac{d_h}{L_f} = \frac{2}{3}\frac{\varepsilon}{(1-\varepsilon)^{2/3}} \tag{7}$$

Allen [6] found that the size dependent frictional fraction for the tested rocks should be x_f=0.45 to fit his thermal experiments, so this value is used in this study as well.

The dependency of the Hagen number *Hg* on the pressure drop shows how important the flow characteristics are for the heat transfer in a packed bed. Equation 8 by Singh, Saini and Saini [8] features a dependency of the pressure drop on particle shapes which has been compared to experimental data by them and [6].

$$\Delta p = 4.466\, {Re_p}^{-0.2}\psi^{0.696}\varepsilon^{-2.945}e^{11.85\,(\log_{10}\psi)^2}\frac{\Delta x\, G^2}{\rho_f d_p} \tag{8}$$

The storage's heat losses occur on the walls, top and bottom of the tank. Given the marginal prices of insulation material, it seems reasonable to choose insulation thick enough to keep the heat flux low. Because of the large surface area and the high temperatures there, the hot duct must be paid special attention.

4. Idling Mode

Single tank sensible heat storage systems work by storing the material in layers of different temperatures, ideally with a region of high temperature gradients in between the hot and cold phase (thermocline). If this region widens, the effective thermal capacity of the storage decreases and more warm air exits the storage unused. In order to maintain a high temperature gradient even during several hours of standstill, e.g. in a winter night, heat transfer inside the storage has to be minimized.

The chosen Equations (9)-(12) for this process, called destratification, were recommended by Tsotsas and Martin [12]. The heat fluxes between the layers are then calculated according to Fourier's law in one-dimensional form.

$$\lambda_{eff} = \lambda_f \left[1 - \sqrt{1-\varepsilon} + \sqrt{1-\varepsilon} \frac{\lambda_{conduction}}{\lambda_f} \right] \tag{9}$$

$$\lambda_{conduction} = \frac{2\,\lambda_f}{N_{destrat}} \left(\frac{B}{N^2} \frac{\frac{\lambda_s}{\lambda_f} - 1}{\lambda_s} \ln \frac{\lambda_s}{\lambda_f B} - \frac{B+1}{2} - \frac{B-1}{2} \right) \tag{10}$$

$$N_{destrat} = 1 - \frac{B\,\lambda_f}{\lambda_s} \tag{11}$$

$$B = 1.25 \left(\frac{1-\varepsilon}{\varepsilon} \right)^{10/9} \tag{12}$$

5. Validation of the Storage Model

5.1. Pressure Drop

Because the pressure drop is the basis for the used heat transfer correlations, it will be validated first. A simulation of the model has been run with the same input data that Chandra and Willits [13] used for their experiments. Their best-fit correlation is compared to the model in Figure 2. It can be seen, that the predicted pressure drop is generally higher than the measured when Re_p>100. A possible explanation is that at their N value, wall channeling has a more dominant effect due to the relatively large area with a high void fraction. When compared to experiments with wall linings, classic set ups show pressure drops 35 to 45 % lower (see [6]). The data with installed wall linings could be reproduced well by the model.

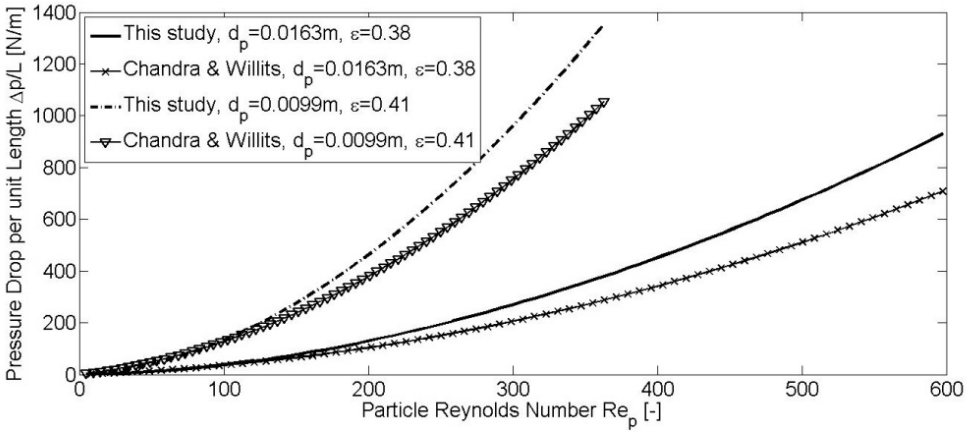

Figure 2: Pressure Drop Validation with Data by Chandra and Willits [13]

5.2. General Heat Transfer

Some of the many - often only slightly - differing correlations in the literature for Nusselt numbers over particle Reynolds numbers are compared to the model in Figure 3. All of them were derived from experimental data by the authors and compared favorable. For example, Chandra and Willits [13] has a mean deviation of only 3.4 % in their best fit curve. The input values for the plot model and calculations are given in the plot's legend. They lie in the respective stated areas of validity.

5.3. Charging/Discharging

The thermocline shapes in the 5.8 m^3 rock bed of Hollands, Sullivan and Shewen [7] could be reproduced well for several hours of charging but the storage appears to be more filled in the model (see Figure 4). The reason for this might lie in insufficient measuring precision at the low temperatures the experiments have been conducted at. Heat losses in the experiment that haven't been accounted for to the right extent could cause the differences in the highest layers. They stated that the temperature difference in one layer were up to 7 K. The shown values of their study are either averaged or center temperatures.

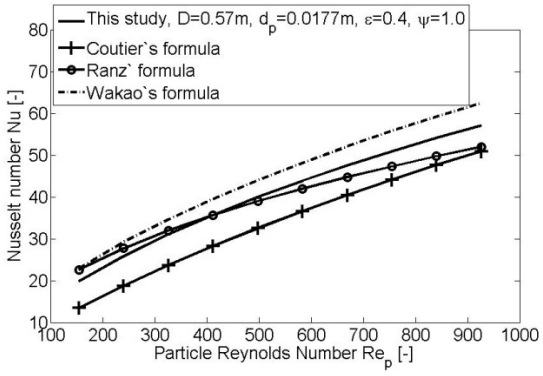

Figure 3: Fluid to particle Nusselt number from different publications [14], [15], [16].

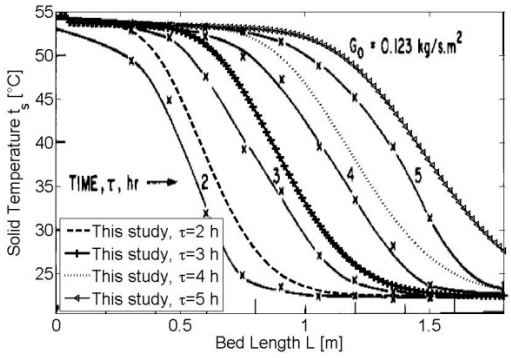

Figure 4: Charging temperature profiles. Plot by Hollands, Sullivan and Shewen [17] with own data.

A set up by Meier and Winkler [10] featured a small tube-to-particle ratio but elevated temperatures. The simulation predicts a better stratification than the actual measurements (see Figure 5a). At an *N* value of only 7, the wall effect could have a noticeable effect on the outcome of the experiments. They also stated that the thermal losses through the wall are 'considerable' but could be reproduced by their model. Due to a lack of detailed information of their insulation, these losses can only be approximated in this study.

They also ran a simulation of a utility size TES for a 30 MW_e CSP plant. Compared to this, the model shows more conservative temperatures but again a better thermocline (see Figure 5b). The overall agreement even after a simulation time of 8 h is good, though. The losses they calculate for the big storage are probably much smaller because of the decreased surface area-to-volume ratio of the tank.

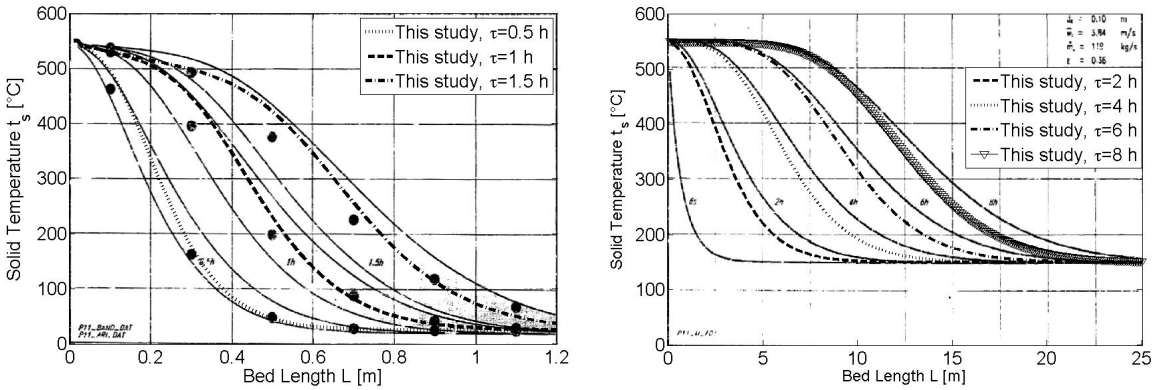

Figure 5 a, b: Measured and simulated temperatures during charging. Plot by Meier and Winkler [10] with own additional data.

To sum up, exactly reproducing every measured charging or discharging temperature curve proves difficult, because the proposed correlations in the literature usually can't describe the experiments in the same paper within a margin of ±10 %. When applied on other author's experimental outcome, the disagreement is almost always very poor. Keeping this in mind, the validation of the analyzed model is satisfactory.

5.4. Destratification

Figure 6 shows the temperature distribution over 70 hours of idling as measured by Jones and Golshekan [18] and as simulated with the model. The agreement is good except for the colder regions of the storage that gain less thermal energy than in the experiment. Most data found on destratification of packed beds is incomplete and couldn't be used for validation. For example in the demonstrated case, the insulation properties had to be guessed.

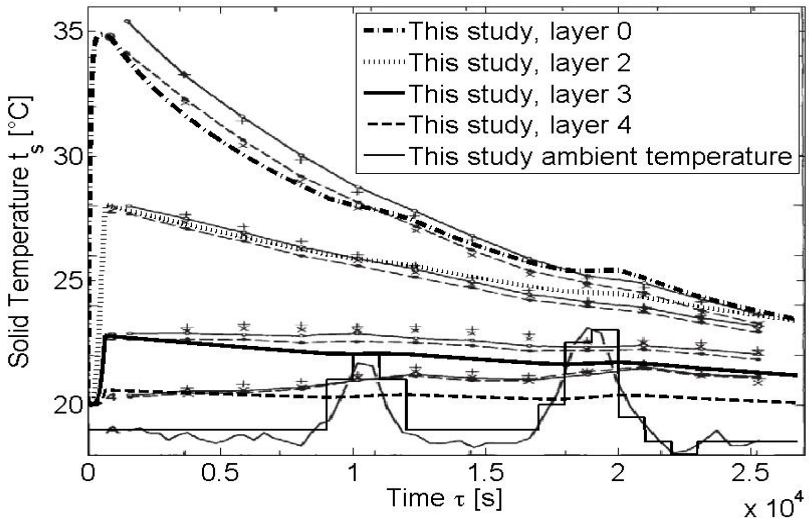

Figure 6: Destratification. Plot by Jones and Golshekan [18] with additional own data.

6. Plant Model

The model of the rest of the plant consists of an hourly demand profile for the plant that is directly derived from grid data for South Africa. This approach is supposed to prove the SUNSPOT cycle's ability to supply base-load power to the grid. The heliostat field, receiver and gas turbine are modeled according to Gauché and Pfenninger [19]. Solar irradiation is implemented by hourly measured data Upington, South Africa. The

exact plant control and therefore heat source (receiver, combustor, storage) for every condition has not been worked out yet. The Rankine cycle is modeled by a simplified efficiency and demand approach. The expected efficiency increase due to shifting cooling to colder night time is accounted for by hourly ambient temperature data.

7. Conclusion/Outlook

The developed storage model has been validated with experimental results from the literature and shows reasonable agreement. However, most of the predicted parameters are in a relatively wide margin of error. This has been expected because of the disagreement between existing studies. Some of the reasons for the unsatisfactory repeatability are scaling effects because of the low tube-to-particle diameter ratios, lack of information for insulation and unknown particle properties. The influence of these uncertainties on a plant-wide simulation has to be shown in a sensitivity analysis once the control algorithms are implemented.

When the whole plant is modeled, sensitivity analyses for the parameters of interest and optimizations for costs and energetic values will be done.

Currently, work is being done on CFD models of rock bed storages. When these become feasible for utility-sized tanks, they could prove or disprove the results of this relatively simple model. Merging them with FEM simulations, the critical question of thermo-mechanical stresses on walls and storage material, which is out of the scope of this project, could be answered as well.

Acknowledgements

The authors would like to express their gratitude to K.G. Allen for his preparatory work and sharing his knowledge.

Works cited

[1] Detlef G. Kröger. (2011, April) [Online]. HYPERLINK "Solar Thermal Energy Research Group" http://blogs.sun.ac.za/sterg/files/2011/05/SUNSPOT-2.pdf

[2] T.E.W. Schumann, "Heat transfer: A liquid flowing through a porous prism," *Journal of the Franklin Institute*, vol. 208, no. 3, pp. 405-416, 1929.

[3] P.J. Hughes, THE DESIGN AND PREDICTED PERFORMANCE OF ARLINGTON HOUSE, 1975.

[4] Kazunobu Sagara and Nobuo Nakahara, "Thermal performance and pressure drop of rock beds with large storage materials," *Solar Energy*, vol. 47, no. 3, pp. 157-163, 1991.

[5] Holger Martin, "The Lévêque-Analogy or How to Predict Heat and Mass Transfer from Fluid Friction," in *HEFAT2005*, Cairo, 2005.

[6] Kenneth Guy Allen, Performance characteristics of packed bed thermal energy storage for solar thermal power plants, 2010.

[7] K. G. T. Hollands, H. F. Sullivan, and E. C. Shewen, "Flow uniformity in rock beds," *Solar Energy*, vol. 32, no. 3, pp. 343-348, 1984.

[8] R. Singh, R. Saini, and J. Saini, "Nusselt number and friction factor correlations for packed bed solar energy storage system having large sized elements of different shapes," *Solar Energy*, vol. 80, no. 7, pp. 760-771, 2006.

[9] Stefan Zunft, Jochim Hahn, and Jannes Kammel, "FLOW DISTRIBUTION CALCULATIONS IN REGENERATOR-TYPE HEAT STORAGE FOR SOLAR TOWER PLANTS," in *SolarPACES*, Granada, 2011.

[10] Anton Meier and Christian Winkler, "Experiment for modelling high temperature rock bed storage," *Solar energy materials*, vol. 24, pp. 255-264, 1991.

[11] B. Eisfeld and K. Schnitzlein, "The influence of confining walls on the pressure drop in packed beds," *Chemical Engineering Science*, vol. 56, no. 41, pp. 4321-4329, 2001.

[12] E. Tsotsas and Holger Martin, "Thermal conductivity of packed beds: A review," *Chemical Engineering and Processing: Process Intensification*, vol. 22, no. 1, pp. 19-37, 1987.

[13] Pitam Chandra and D. Willits, "Pressure drop and heat transfer characteristics of air-rockbed thermal storage systems," *Solar Energy*, vol. 27, no. 6, pp. 547-553, 1981.

[14] J. Pascal Coutier and E. A. Farber, "Two applications of a numerical approach of heat transfer process within rock beds," *Solar Energy*, vol. 29, no. 6, pp. 451-462, 1982.

[15] Shriniwas S. Chauk and Liang-Shih Fan, "Heat Transfer in Packed and Fluidized Beds," in *Handbook of Heat Transfer*.: McGraw-Hill, 1998.

[16] N. Wakao and T. Funazkri, "Effect of fluid dispersion coefficients on particle-to-fluid mass transfer coefficients in packed beds," *Chemical Engineering Science*, vol. 33, no. 10, pp. 1375-1384, 1978.

[17] H. F. Sullivan, K. G. T. Hollands, and E. C. Shewen, "Thermal destratification in rock beds," *Sullivan, H. F.*, vol. 33, no. 2, pp. 227-229, 1984.

[18] Barrie W. Jones and Mahyar Golshekan, "Destratification and other properties of a packed bed heat store," *International Journal of Heat and Mass Transfer*, vol. 32, no. 2, pp. 351-359, 1989.

[19] Paul Gauché and Stefan Pfenninger, Personal Communication, Feb. 28, 2012.